ORIGINAL RESEARCH

Circulating MicroRNAs in Delayed Cerebral Infarction After Aneurysmal Subarachnoid Hemorrhage

Gang Lu, MD, PhD; Man Sze Wong, MSc; Mark Zhi Qiang Xiong, PhD; Chi Kwan Leung, PhD; Xian Wei Su, PhD; Jing Ye Zhou, PhD; Wai Sang Poon, MD; Vera Zhi Yuan Zheng, MSc; Wai Yee Chan, PhD; George Kwok Chu Wong, MD

***Background*—**Delayed cerebral infarction (DCI) is a major cause of morbidities after aneurysmal subarachnoid hemorrhage (SAH) and typically starts at day 4 to 7 after initial hemorrhage. MicroRNAs (miRNAs) play an important role in posttranscriptional gene expression control, and distinctive patterns of circulating miRNA changes have been identified for some diseases. We aimed to investigate miRNAs that characterize SAH patients with DCI compared with those without DCI.

***Methods and Results*—**Circulating miRNAs were collected on day 7 after SAH in healthy, SAH-free controls (n=20), SAH patients with DCI (n=20), and SAH patients without DCI (n=20). We used the LASSO (least absolute shrinkage and selection operator) method of regression analysis to characterize miRNAs associated with SAH patients with DCI compared with those without DCI. In the 28 dysregulated miRNAs associated with DCI and SAH, we found that a combination of 4 miRNAs (miR-4532, miR-4463, miR-1290, and miR-4793) could differentiate SAH patients with DCI from those without DCI with an area under the curve of 100% (95% CI 1.000–1.000, $P<0.001$). This 4-miRNA combination could also distinguish SAH patients with or without DCI from healthy controls with areas under the curve of 99.3% (95% CI 0.977–1.000, $P<0.001$) and 82.0% (95% CI 0.685–0.955, $P<0.001$), respectively.

***Conclusions*—**We found a 4-miRNA combination that characterized SAH patients with DCI. The findings could guide future mechanistic study to develop therapeutic targets. **(*J Am Heart Assoc*. 2017;6:e005363. DOI: 10.1161/JAHA.116.005363.)**

Key Words: biomarker • delayed cerebral infarction • miRNA • stroke • subarachnoid hemorrhage

Aneurysmal subarachnoid hemorrhage (SAH) accounts for about 3% to 5% of stroke and is an important cause of stroke in young populations, causing significant socioeconomic burden worldwide.[1] Up to two thirds of SAH patients experience cognitive impairment and impaired quality of life and may not be able to return to their previous work.[2–8]

Delayed cerebral infarction (DCI) occurs in up to 44% of SAH patients and typically starts at day 4 to 7 after the initial hemorrhage.[9–11] DCI is a well-established and relevant clinical surrogate marker for neurological outcome after SAH.[12] Numerous factors including age, initial neurological impairment, intraventricular hemorrhage, SAH load, and aneurysm size are reported to be associated with the development of DCI.[13–16]

MicroRNAs (miRNAs) are a family of small (19–23 base pairs), noncoding, and deeply conserved RNA molecules that regulate target gene expression at a posttranscriptional level by inhibiting mRNA translation[17] or destabilizing mRNA molecules.[18] There are 1881 miRNAs in human genomes, 296 of which are currently annotated as *high confidence*, according to miRBase 21.0.[19] Circulating miRNAs have been demonstrated to be promising diagnostic or prognostic biomarkers for cerebrovascular conditions such as myocardial infarction,[20] atherosclerotic diseases,[21] stroke,[22] cerebral infarction,[23] hypertension,[24] intracranial aneurysms,[25–28] and SAH.[29,30]

From the Division of Neurosurgery, Department of Surgery, Prince of Wales Hospital (G.L., J.Y.Z., W.S.P., V.Z.Y.Z., G.K.C.W.) and CUHK-SDU Joint Laboratory on Reproductive Genetics, School of Biomedical Sciences (G.L., M.S.W., W.Y.C.), The Chinese University of Hong Kong, China; Bioinformatics Unit, SDIVF R&D Centre, Hong Kong Science and Technology Parks, Hong Kong, China (M.Z.Q.X., C.K.L., X.W.S.).

Accompanying Tables S1 and S2 are available at http://jaha.ahajournals.org/content/6/4/e005363/DC1/embed/inline-supplementary-material-1.pdf

Correspondence to: George Kwok Chu Wong, MD, 4/F, Department of Surgery, Lui Che Woo Clinical Sciences Building, Prince of Wales Hospital, 30-32 Ngan Shing Street, Shatin, NT, Hong Kong, China. E-mail: georgewong@surgery.cuhk.edu.hk

Received January 7, 2017; accepted March 17, 2017.

In the current study, we aimed to investigate miRNAs that characterized SAH patients with DCI compared with those without DCI.

Methods

Patient Recruitment and Sample Collection

The study was approved by the Joint NTEC-CUHK (New Territories East Cluster-Chinese University of Hong Kong) Clinical Research Ethics Committee, and written informed consent was obtained from all participants or their next of kins. Circulating miRNAs were collected from healthy controls (n=20), SAH patients with DCI (n=20) at day 7 after SAH, and SAH patients without DCI (n=20) at day 7 after SAH. SAH patients were recruited from Prince of Wales Hospital, Chinese University of Hong Kong, Hong Kong Special Administrative Region, People's Republic of China, between 2012 and 2013. Ruptured cerebral aneurysms were diagnosed by computer tomography angiography. For SAH patients, the healthy controls (n=20) were recruited from the family members of SAH patients with the no major medical problem (including no smoking history and hypertension). Participant characteristics are shown in Table 1.

Table 1. Participant Characteristics

	Control (n=20)	SAH With DCI (n=20)	SAH Without DCI (n=20)	*P* Value
Demographics				
Age, y	50±17	59±12	59±11	
Female, %	65 (13)	45 (9)	65 (13)	
WFNS grade on admission, %				
1–2	···	60 (12)	75 (15)	0.311
3–5	···	40 (8)	25 (5)	
CT feature on admission				
Fisher grade 3/4, %	···	100 (20)	100 (20)	1.000
Risk factors, %				
Hypertension	···	55 (11)	30 (6)	0.200
Smokers	···	10 (2)	0 (0)	0.487
Outcome				
Infarction, %	···	65 (13)	0 (0)	<0.001*
mRS 3 mo, median	···	2	1	0.034*
mRS 3 mo, >2	···	45 (9)	15 (3)	0.082
mRS 3 mo, ≤2	···	55 (11)	85 (17)	

Data are % (N), mean±SD, or median. CT indicates computed tomography; DCI, delayed cerebral infarction; mRS 3 mo, modified Rankin Scale 3-month; SAH, subarachnoid hemorrhage; WFNS, World Federation of Neurosurgical Societies.
*P<0.05.

Delayed Cerebral Infarction

DCI is defined as a new cerebral infarction identified on computed tomography after exclusion of procedure-related infarctions.[3,12] Procedure-related infarction was defined as new hypodensity appearing on the posttreatment computed tomography at 12 to 24 hours after aneurysm treatment. All recruited patients had delayed computed tomography of the brain at 2 to 3 weeks after presentation available for assessment. The diagnoses of DCI were made by consensus of 2 neuroradiologists.

Quantitative Polymerase Chain Reaction

Peripheral blood samples were obtained using EDTA tubes with standard procedures. Samples were placed on ice immediately and centrifuged at 1000*g* for 15 minutes at 4°C. Plasma fraction was aliquoted and stored at −80°C. RNA isolation and quantitative real-time polymerase chain reaction were performed, as described previously.[29] Briefly, serum was prepared by adding 20% wt/vol $CaCl_2$ (Sigma-Aldrich) into the plasma samples at a ratio of 1:100, followed by clotting overnight and centrifugation. Total RNA was isolated from pooled serum samples using the miRNeasy Serum/Plasma Kit following the manufacturer's instructions (Qiagen). The quantity of the extracted RNA was determined using a Nanodrop 2000 UV-Vis spectrophotometer (Thermo Scientific). The results were analyzed with the Applied Biosystems SDS software for Ct values and melting curve analyses. Of the 99 possible deregulated miRNAs associated with SAH,[29] we selected the top 20 differentially regulated miRNAs between SAH patients with and without DCI; the top 8 miRNAs between SAH patients with DCI and healthy controls (2 overlapped); and miR-132-3p and miR-324-3p, the 2 previously reported circulating miRNAs in SAH patients[29] from a total of 28 unique miRNAs for expression analysis. Table S1 is the list of quantitative polymerase chain reaction primers for miRNA expression profiling used in this study.

Statistical Analyses

Heat maps with hierarchical clustering and principal component analysis (PCA) were computed and visualized using the functions *pHeatmap* and *prcomp*, respectively, from the stats package for R version 3.0.1 (R Foundation for Statistical Computing). The R package pROC was used to plot and visualize receiver operating characteristic (ROC) curves to compute the area under the curve (AUC) and confidence intervals to evaluate the performance of the miRNA-based

classifier.[31] Different R packages and functions were used to construct the 4 classification models to identify the miRNA-based classifiers that could differentiate SAH patients with or without DCI after SAH—the linear support vector machine (R package e1071, function svm, kernel="linear"), nonlinear support vector machine (R package e1071, function svm, kernel="radial"), linear discriminant analysis (R package MASS, function lda), and logistic regression (R package stats, function glm, family="binomial")—as previously described.[32] The R package glmnet was used to fit the LASSO (least absolute shrinkage and selection operator) regression model via penalized maximum likelihood to define the miRNA-based classifier.[33] The value λ=0.07765104 based on cross-validation, and *t* tests were used to compute the *P* value (Tables 1 and 2). A value of $P<0.05$ was regarded as statistically significant.

Results

Hierarchical Clustering of miRNAs Associated With SAH With and Without DCI

We performed unsupervised hierarchical clustering to graphically represent the averaged microarray expressions of the 28 miRNAs derived from the 3 cohorts for exploratory analysis: healthy controls, SAH with DCI, and SAH without DCI. The dendrogram represented with the heat map showing the entire data matrix of the 3 cohorts indicated that the expression profiles of the 28 miRNAs among the 3 cohorts are distinctive, with clear cluster dissimilarity (results not shown), and suggested that a subset of the 28 miRNAs could characterize SAH patients with DCI from those without DCI.

We next performed quantitative polymerase chain reaction array analyses to quantify the expression levels of the 28 SAH-associated miRNAs (Figure 1A) and used PCA for pattern recognition to evaluate the distance connectivity of the 2 SAH subtypes (Figure 1B). PCA generated 2 distinct clusters with minimal overlap of the 2 SAH subtypes, highlighting the possibility of characterizing the disease subtypes using a miRNA combination.

miRNAs That Characterized SAH With DCI

Given the distinctive pattern of miRNA expression profile between the 2 SAH subtypes, we initially evaluated the performance of individual miRNAs to characterize SAH patients with and without DCI using ROC analysis.[34] Based on the sensitivity (true-positive rate) and specificity (false-positive rate) at varied threshold levels, the ROC analysis allowed us to select possibly optimal models for DCI discrimination.

We plotted the ROC curves for individual miRNAs from a total of 28 miRNAs according to their quantitative polymerase chain reaction–measured expression levels in the SAH groups with DCI and without DCI. The results are shown in Table 2. The AUCs of 8 miRNAs can achieve >85% ($P<0.0005$), and 4 of them—miR-4532, miR-4793, miR-1290, and miR-421—are >90%. For miR-1290, the AUC, specificity, and sensitivity were 95.3% (95% CI 0.897–1), 0.900, and 0.850, respectively, at a cutoff level of 8.653.

We postulated that a combination of miRNAs would show characteristics for SAH with versus without DCI. We examined each miRNA combination of the 28 SAH-associated miRNAs, based on their sensitivity, specificity, and accuracy, using the 4 different classifier algorithms: linear support vector machine, nonlinear support vector machine, linear discriminant analysis, and logistic regression. The results are shown

Table 2. Performance of Individual MicroRNAs in Subarachnoid Hemorrhage Subtypes Classification

miRNA	AUC (95% CI)	*P* Value
miR-4532	0.9475 (0.873–1.000)	1.80E-08
miR-4793	0.93 (0.584–1.000)	2.14E-07
miR-1290	0.9525 (0.897–1.000)	3.54E-07
miR-421	0.9175 (0.836–0.999)	3.24E-06
miR-4492	0.895 (0.798–0.992)	7.26E-06
miR-574	0.8625 (0.753–0.972)	2.70E-05
miR-4689	0.86 (0.748–0.972)	2.87E-05
miR-4449	0.855 (0.741–0.969)	3.16E-05
miR-93-5p	0.835 (0.713–0.957)	9.31E-05
miR-1268	0.795 (0.648–0.942)	2.69E-04
miR-4497	0.8175 (0.685–0.950)	3.77E-04
miR-3178	0.7875 (0.640–0.935)	6.71E-04
miR-4674	0.765 (0.602–0.928)	7.94E-04
miR-297	0.81 (0.671–0.949)	9.15E-04
miR-4463	0.815 (0.677–0.953)	1.03E-03
miR-4690	0.7325 (0.568–0.897)	5.38E-03
miR-4459	0.73 (0.560–0.900)	9.75E-03
miR-3651	0.705 (534–0.876)	1.99E-02
miR-132	0.7125 (0.547–0.878)	2.37E-02
miR-4433	0.67 (0.497–0.843)	7.86E-02
miR-339-5p	0.6625 (0.490–0.835)	7.95E-02
miR-125a	0.66 (0.483–0.837)	1.58E-01
miR-324	0.59875 (0.419–0.779)	2.29E-01
miR-4440	0.5675 (0.385–0.750)	4.16E-01
miR-4454	0.5075 (0.321–0.694)	7.66E-01
miR-27b	0.49 (0.304–0.676)	8.62E-01
miR-27a	0.485 (0.299–0.671)	9.24E-01
miR-15a	0.525 (0.339–0.711)	9.52E-01

AUC indicates area under the receiver operating characteristic curve.

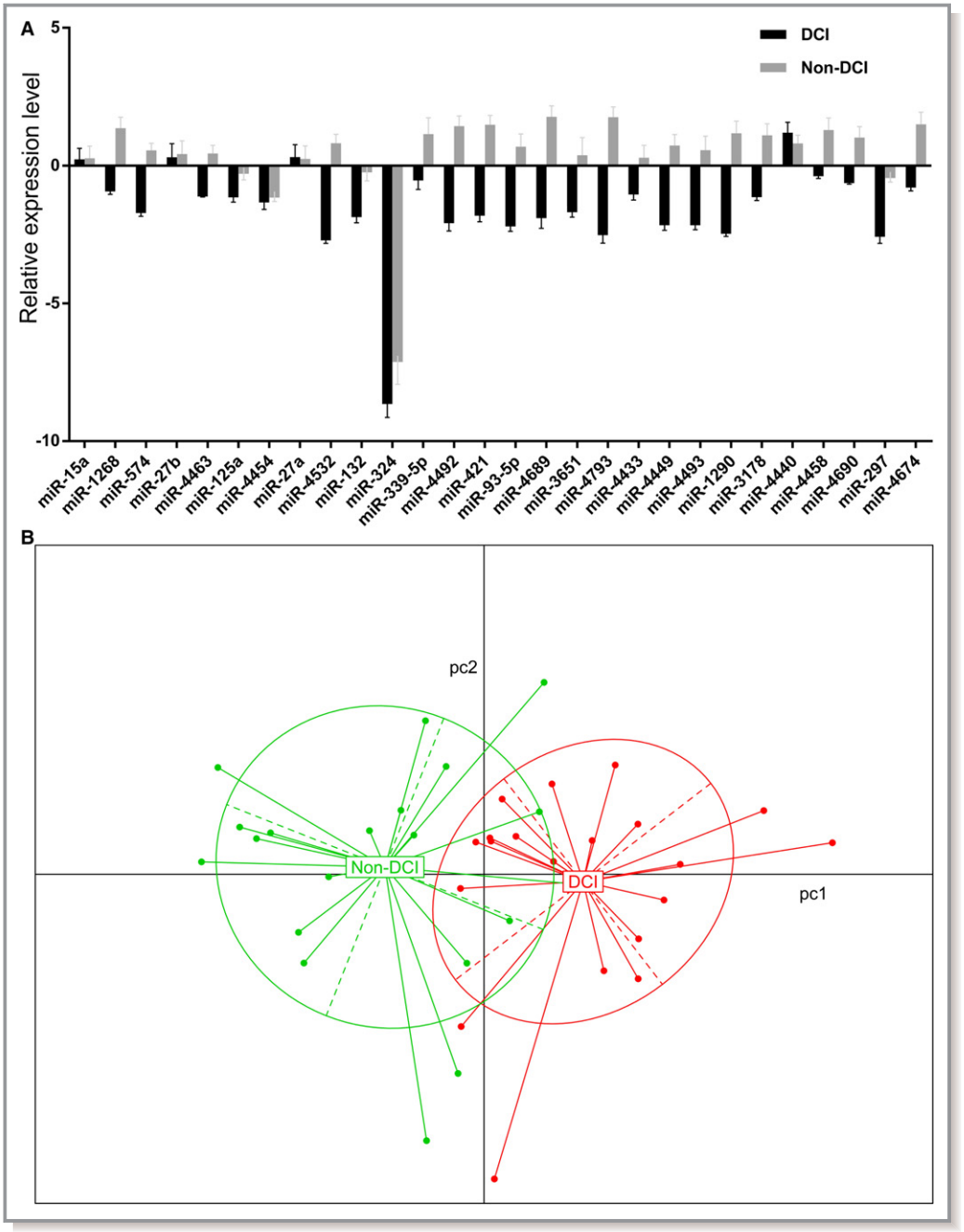

Figure 1. A, Quantitative polymerase chain reaction array of the 28 subarachnoid hemorrhage (SAH)-associated microRNAs. The expression levels were normalized to the control and expressed as ΔΔCt. B, Principal component analysis of the 2 SAH subtypes with or without delayed cerebral infarction (DCI).

in Figure 2. All 3 readouts improved while increasing the number of miRNAs contained in each classifier.

We next performed the LASSO regression analysis involving penalizing the absolute size of the regression coefficients to determine the accuracy using a combination of miRNAs to distinguish SAH with and without DCI (Figure 3A). The results are shown in Figure 3B. ROC analysis indicated that the AUC achieved 100% (95% CI 1–1, $P<0.0001$) using 4 miRNAs, namely, miR-4463, miR-4532, miR-4793, and miR-1290, according to the LASSO regression model and the ROC analysis using the following formula: $\ln(Y/1-Y)=-4.29759355+$ miR-4463$\times$0.16589606+miR-4532$\times$0.43352951+miR-4793$\times$ 0.09569081+miR-1290$\times$0.2602013. PCA analysis indicated that the 4-miRNA combination could produce 2 nonoverlapping clusters to unambiguously differentiate SAH with and without DCI.

Interestingly, the 4 miRNAs were strongly repressed in SAH blood samples with DCI but activated in the non-DCI

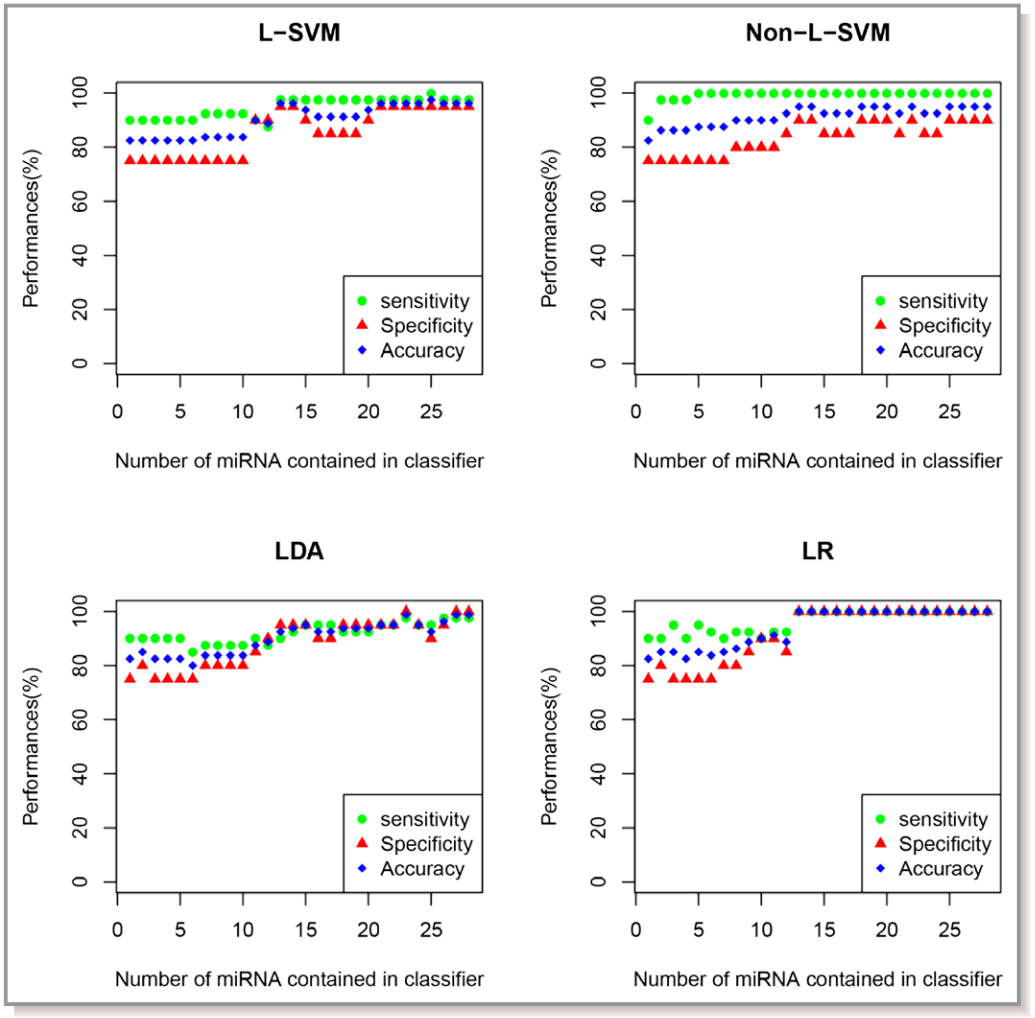

Figure 2. Four classification models, namely, linear support vector machine (L-SVM), nonlinear support vector machine (non-L-SVM), linear discriminant analysis (LDA), and logistic regression (LR) models, were applied to construct microRNA (miRNA) classifiers. The performance of the miRNA-based classifiers was determined by leave-one-out cross-validation. The *x*-axis denotes the number of miRNAs contained in the classifier, whereas the *y*-axis indicates the performance of the classifiers including sensitivity (green circle), specificity (blue square), and accuracy (red triangle). In each group with the same miRNA number, only the classifier displaying the best performance is presented.

samples compared with healthy controls (Figure 4). The biphasic expressions of these 4 miRNAs in the SAH patients with or without DCI also provided discrimination with an AUC >80% by ROC analyses to differentiate the SAH patients with or without DCI from healthy controls with AUCs of 99.3% (95% CI 0.977–1, $P<0.0001$) and 82.0% (95% CI 0.685–0.955, $P<0.0005$), respectively. The results supported the disease-specific nature of the 4 miRNAs.

Discussion

In this study, both the heat map and PCA analysis suggested that a combination of miRNAs could characterize SAH patients with DCI from those without DCI (Figure 1). We demonstrated that a number of miRNAs could offer good to excellent discriminatory power between SAH with and without DCI (Table 2). LASSO regression analysis and PCA analysis further demonstrated that a 4-miRNA combination (miR-4463, miR-4532, miR-4793, and miR-1290) could produce 2 nonoverlapping clusters to unambiguously differentiate SAH with and without DCI, with an AUC of 100% (95% CI 1–1, $P<0.0001$) (Figure 3). In addition, the classifier can also distinguish the healthy controls from each SAH subtype with or without DCI (Figure 4), highlighting its disease specificity.

Recently, studies of miRNAs in serum and cerebrospinal fluid identified biomarkers associated with occurrence of SAH, including miR-92a, let-7b, miR-204-5p, miR-223-3p, miR-337-5p, miR-451a, miR-489, miR-508-3p, miR-514-3p, miR-516-5p,

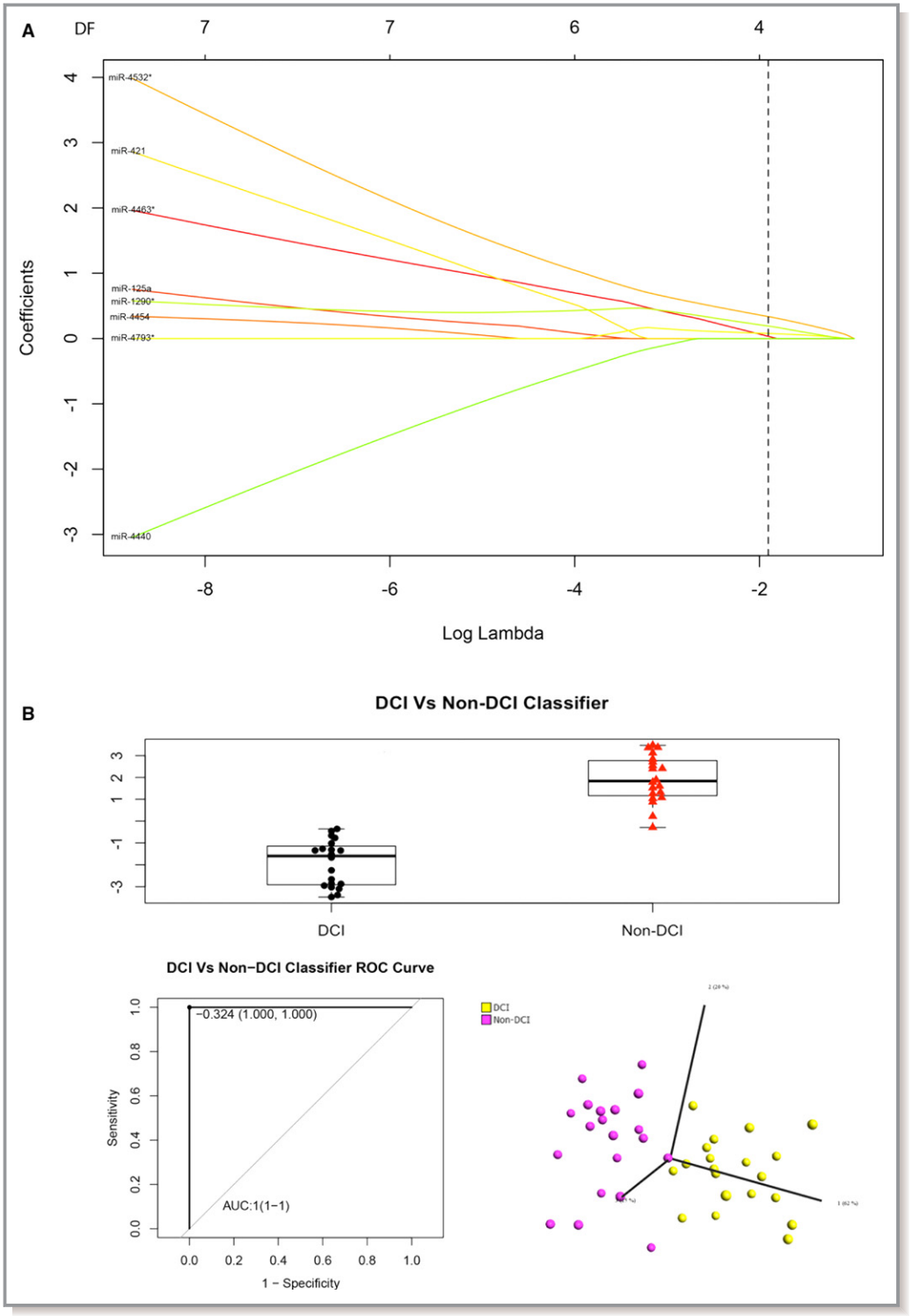

Figure 3. A, LASSO (least absolute shrinkage and selection operator) regression analysis, (B) the box-and-whisker plot (upper panel), receiver operating characteristic (ROC) curve (bottom left panel), and principal component analysis (bottom right panel) of the 4 microRNAs (miR-4532, miR-4463, miR-1290, and miR-4793-3p) in the subarachnoid hemorrhage groups with and without delayed cerebral infarction (DCI) in the classification algorithm. AUC indicates area under the curve.

miR-548, miR-599, miR-937, miR-1224-3p and miR-1301.[29,35,36] Our previous genomewide serum miRNA expression profiling also suggested that miR-132-3p and miR-324-3p could be potential biomarkers for SAH.[29,35,36] Styllis and others investigated cerebrospinal fluid miRNAs in 10 SAH patients with and 10 without cerebral vasospasm and identified miR-

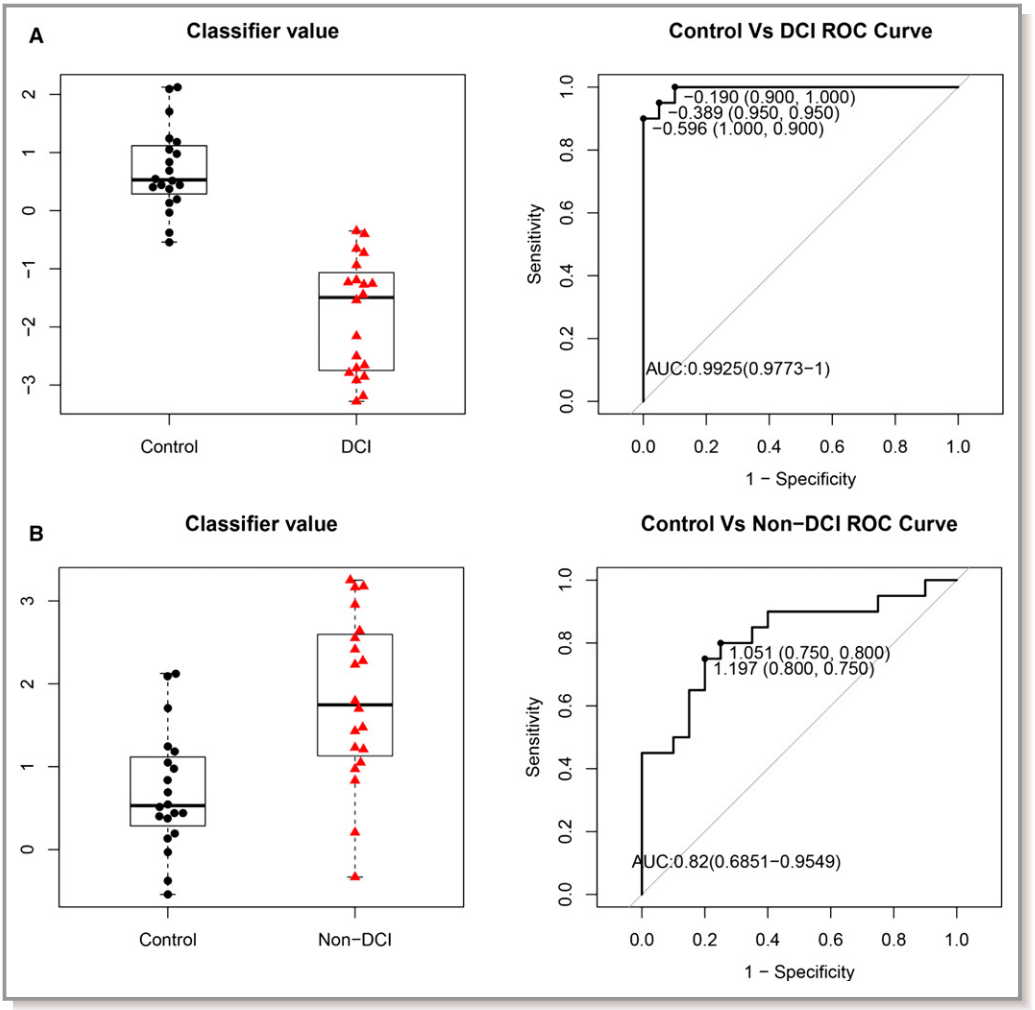

Figure 4. Box-and-whisker plots (left panel) and receiver operating characteristic curves (right panel) of the 4 microRNAs (miR-4532, miR-4463, miR-1290, and miR-4793-3p) in (A) subarachnoid hemorrhage (SAH) patients with delayed cerebral infarction (DCI) vs control and (B) SAH patients without DCI (non-DCI) vs control, using the R package. AUC indicates area under the curve.

27a-3p, miR-516a-5p, miR-566, and miR-1197 as potential biomarkers for cerebral vasospasm but not DCI.[36] The identification of miRNAs associated with DCI after SAH has been understudied, hindering understanding and development of therapeutic strategies for DCI after SAH.

Given that the downstream targets and functional specificities of the 4 miRNAs (miR-4463, miR-4532, miR-4793 and miR-1290) are uncharacterized, we performed gene-centric analysis to identify their common and unique potential targets using 3 algorithms: TargetScan, miRanda, and PITA. Considerable overlaps of their downstream targets were shared by these 4 miRNAs, inferring that these miRNAs may act on common regulatory pathways mediated by their shared targets for the development of DCI after SAH (Figure 5). KEGG (Kyoto Encyclopedia of Genes and Genomes) and gene ontology analyses also consistently revealed that the targets of these 4 miRNAs associated with multiple developmental pathways including Wnt signaling pathway, hedgehog and oxytocin signaling pathways. These pathways are broadly involved in neurogenesis and nervous system development, suggesting that these 4 miRNAs may function as causative factors in DCI pathology associated with SAH (Table S2).

The 4 novel miRNAs—miR-4463, miR-4532, miR-4793, and miR-1290—have not been associated with SAH pathology. miR-4532 has been associated with breast cancer cell chemotherapy resistance.[37] miR-4793 expression was elevated in liver metastases of sporadic colorectal cancer patients.[38] miR-1290 has been widely associated with different types of cancers including colorectal cancer, cervical cancer, non–small cell lung cancer, breast cancer, hepatocellular carcinoma, gastric cancer, laryngeal carcinoma, lymphoblastic leukemia, esophageal squamous cell carcinoma, lung adenocarcinoma, prostate cancer, pancreatic cancer, and bladder carcinoma, as well as oral submucosal fibrosis, nonalcoholic

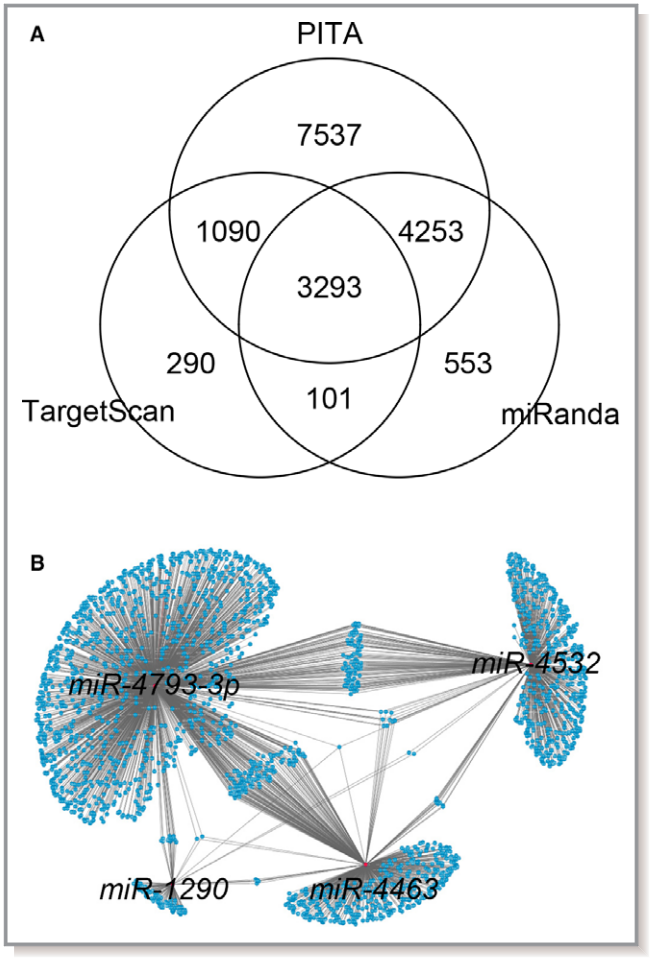

Figure 5. A, Gene-centric analysis of the putative targets of the 4 microRNAs (miRNAs; miR-4532, miR-4463, miR-1290, and miR-4793-3p) using TargetScan, miRanda, and PITA. B, Topological network view of the downstream targets shared by the 4 miRNAs, constructed by Cytoscape.

fatty liver disease, and chronic rhinosinusitis.[39–41] miR-4463 has been shown to serve as a biomarker for a common female reproductive disease called *polycystic ovary syndrome* and arteriosclerosis obliterans.[42,43]

Our current study had several limitations. First, our SAH-associated miRNA pools were obtained from patients at day 7 after SAH, which is a commonly reported time point for etiological study of DCI. Time-course expression profiling of serum miRNAs in SAH patients at multiple time points could investigate stage/time-specific miRNAs for SAH with or without DCI in future. Second, the current study did not investigate the pathophysiological roles of these miRNAs in DCI after SAH and propose therapeutic targets. Third, the sample size was small, and subgroup analyses such as admission neurological grade and the mode of aneurysm treatment were not performed. In addition, the sample size did not allow meaningful matched group analyses. Fourth, 28 miRNAs were selected to find the important miRNAs involved to guide further mechanistic study to find therapeutic targets. Fifth, there could be a limitation in diagnosing DCI with computed tomography hypodensity, as magnetic resonance imaging was not routinely performed in our patients. Sixth, validation with another patient cohort would be warranted to confirm our findings. Seventh, cerebrospinal fluid samples were not collected for miRNA analysis and should be considered in future study.

Our work was important as it provides an understanding of the characteristics of circulating miRNAs associated with DCI after SAH. The 4 miRNAs might play distinct roles in DCI after SAH. Further investigations into their roles might bring new therapeutic targets for DCI after SAH. Future time-course studies of miRNAs might also identify SAH patients at risk of subsequent DCI development for stringent monitoring in neurocritical care units and timely treatment.

Conclusions

We found a 4-miRNA combination (miR-4532, miR-4463, miR-1290, and miR-4793) that characterized SAH patients with DCI. The findings could guide future mechanistic study to develop therapeutic targets.

Sources of Funding

This work was supported by the Chinese University of Hong Kong Direct Grant for Research (MD11782) and a collaborative funding from SDIVF R&D Centre.

Disclosures

None.

References

1. Lovelock CE, Rinkel GJ, Rothwell PM. Time trends in outcome of subarachnoid hemorrhage: population-based study and systematic review. *Neurology*. 2010;74:1494–1501.
2. Al-Khindi T, Macdonald RL, Schweizer TA. Cognitive and functional outcome after aneurysmal subarachnoid hemorrhage. *Stroke*. 2010;41:e519–e536.
3. Wong GK, Lam S, Ngai K, Wong A, Mok V, Poon WS; Cognitive Dysfunction after Aneurysmal Subarachnoid Haemorrhage I. Evaluation of cognitive impairment by the montreal cognitive assessment in patients with aneurysmal subarachnoid haemorrhage: prevalence, risk factors and correlations with 3 month outcomes. *J Neurol Neurosurg Psychiatry*. 2012;83:1112–1117.
4. Wong GK, Poon WS, Boet R, Chan MT, Gin T, Ng SC, Zee BC. Health-related quality of life after aneurysmal subarachnoid hemorrhage: profile and clinical factors. *Neurosurgery*. 2011;68:1556–1561; discussion 1561.
5. Scott RB, Eccles F, Molyneux AJ, Kerr RS, Rothwell PM, Carpenter K. Improved cognitive outcomes with endovascular coiling of ruptured intracranial aneurysms: neuropsychological outcomes from the International Subarachnoid Aneurysm Trial (ISAT). *Stroke*. 2010;41:1743–1747.
6. Wong GK, Wun TAM YY, Zhu XL, Poon WS. Incidence and mortality of spontaneous subarachnoid hemorrhage in Hong Kong from 2002 to 2010: a Hong Kong hospital authority clinical management system database analysis. *World Neurosurg*. 2014;81:552–556.
7. de Rooij NK, Linn FH, van der Plas JA, Algra A, Rinkel GJ. Incidence of subarachnoid haemorrhage: a systematic review with emphasis on region, age, gender and time trends. *J Neurol Neurosurg Psychiatry*. 2007;78:1365–1372.

8. Passier PE, Visser-Meily JM, Rinkel GJ, Lindeman E, Post MW. Life satisfaction and return to work after aneurysmal subarachnoid hemorrhage. *J Stroke Cerebrovasc Dis*. 2011;20:324–329.
9. Schmidt JM, Rincon F, Fernandez A, Resor C, Kowalski RG, Claassen J, Connolly ES, Fitzsimmons BF, Mayer SA. Cerebral infarction associated with acute subarachnoid hemorrhage. *Neurocrit Care*. 2007;7:10–17.
10. Dorsch NW, King MT. A review of cerebral vasospasm in aneurysmal subarachnoid haemorrhage part I: incidence and effects. *J Clin Neurosci*. 1994;1:19–26.
11. Ionita CC, Baker J, Graffagnino C, Alexander MJ, Friedman AH, Zaidat OO. Timing of symptomatic vasospasm in aneurysmal subarachnoid hemorrhage: the effect of treatment modality and clinical implications. *J Stroke Cerebrovasc Dis*. 2010;19:110–115.
12. Vergouwen MD, Vermeulen M, van Gijn J, Rinkel GJ, Wijdicks EF, Muizelaar JP, Mendelow AD, Juvela S, Yonas H, Terbrugge KG, Macdonald RL, Diringer MN, Broderick JP, Dreier JP, Roos YB. Definition of delayed cerebral ischemia after aneurysmal subarachnoid hemorrhage as an outcome event in clinical trials and observational studies: proposal of a multidisciplinary research group. *Stroke*. 2010;41:2391–2395.
13. Sundt TM Jr, Piepgras DG, Fode NC, Meyer FB. Giant intracranial aneurysms. *Clin Neurosurg*. 1991;37:116–154.
14. Kassell NF, Torner JC, Jane JA, Haley EC Jr, Adams HP. The international cooperative study on the timing of aneurysm surgery. Part 2: surgical results. *J Neurosurg*. 1990;73:37–47.
15. Rabinstein AA, Friedman JA, Weigand SD, McClelland RL, Fulgham JR, Manno EM, Atkinson JL, Wijdicks EF. Predictors of cerebral infarction in aneurysmal subarachnoid hemorrhage. *Stroke*. 2004;35:1862–1866.
16. Dority JS, Oldham JS. Subarachnoid hemorrhage: an update. *Anesthesiol Clin*. 2016;34:577–600.
17. Guo H, Ingolia NT, Weissman JS, Bartel DP. Mammalian microRNAs predominantly act to decrease target mRNA levels. *Nature*. 2010;466:835–840.
18. Carthew RW, Sontheimer EJ. Origins and mechanisms of miRNAs and siRNAs. *Cell*. 2009;136:642–655.
19. Kozomara A, Griffiths-Jones S. miRBase: annotating high confidence microRNAs using deep sequencing data. *Nucleic Acids Res*. 2014;42:D68–D73.
20. Li C, Chen X, Huang J, Sun Q, Wang L. Clinical impact of circulating miR-26a, miR-191, and miR-208b in plasma of patients with acute myocardial infarction. *Eur J Med Res*. 2015;20:58.
21. Araldi E, Chamorro-Jorganes A, van Solingen C, Fernandez-Hernando C, Suarez Y. Therapeutic potential of modulating microRNAs in atherosclerotic vascular disease. *Curr Vasc Pharmacol*. 2015;13:291–304.
22. Leung LY, Chan CP, Leung YK, Jiang HL, Abrigo JM, Wang de F, Chung JS, Rainer TH, Graham CA. Comparison of miR-124-3p and miR-16 for early diagnosis of hemorrhagic and ischemic stroke. *Clin Chim Acta*. 2014;433:139–144.
23. Zhou J, Zhang J. Identification of miRNA-21 and miRNA-24 in plasma as potential early stage markers of acute cerebral infarction. *Mol Med Rep*. 2014;10:971–976.
24. Heggermont WA, Heymans S. MicroRNAs are involved in end-organ damage during hypertension. *Hypertension*. 2012;60:1088–1093.
25. Jin H, Li C, Ge H, Jiang Y, Li Y. Circulating microRNA: a novel potential biomarker for early diagnosis of intracranial aneurysm rupture a case control study. *J Transl Med*. 2013;11:296.
26. Li P, Zhang Q, Wu X, Yang X, Zhang Y, Li Y, Jiang F. Circulating microRNAs serve as novel biological markers for intracranial aneurysms. *J Am Heart Assoc*. 2014;3:e000972. DOI: 10.1161/JAHA.114.000972.
27. Liu D, Han L, Wu X, Yang X, Zhang Q, Jiang F. Genome-wide microRNA changes in human intracranial aneurysms. *BMC Neurol*. 2014;14:188.
28. Jiang Y, Zhang M, He H, Chen J, Zeng H, Li J, Duan R. microRNA/mRNA profiling and regulatory network of intracranial aneurysm. *BMC Med Genomics*. 2013;6:36.
29. Su XW, Chan AH, Lu G, Lin M, Sze J, Zhou JY, Poon WS, Liu Q, Zheng VZ, Wong GK. Circulating microRNA 132-3p and 324-3p profiles in patients after acute aneurysmal subarachnoid hemorrhage. *PLoS One*. 2015;10:e0144724.
30. Muller AH, Povlsen GK, Bang-Berthelsen CH, Kruse LS, Nielsen J, Warfvinge K, Edvinsson L. Regulation of microRNAs miR-30a and miR-143 in cerebral vasculature after experimental subarachnoid hemorrhage in rats. *BMC Genomics*. 2015;16:119.
31. Robin X, Turck N, Hainard A, Tiberti N, Lisacek F, Sanchez JC, Muller M. pROC: an open-source package for R and S+ to analyze and compare ROC curves. *BMC Bioinformatics*. 2011;12:77.
32. Lin XJ, Chong Y, Guo ZW, Xie C, Yang XJ, Zhang Q, Li SP, Xiong Y, Yuan Y, Min J, Jia WH, Jie Y, Chen MS, Chen MX, Fang JH, Zeng C, Zhang Y, Guo RP, Wu Y, Lin G, Zheng L, Zhuang SM. A serum microRNA classifier for early detection of hepatocellular carcinoma: a multicentre, retrospective, longitudinal biomarker identification study with a nested case-control study. *Lancet Oncol*. 2015;16:804–815.
33. Friedman J, Hastie T, Tibshirani R. Regularization paths for generalized linear models via coordinate descent. *J Stat Softw*. 2010;33:1–22.
34. Hajian-Tilaki K. Receiver operating characteristic (ROC) curve analysis for medical diagnostic test evaluation. *Caspian J Intern Med*. 2013;4:627–635.
35. Powers CJ, Dickerson R, Zhang SW, Rink C, Roy S, Sen CK. Human cerebrospinal fluid microRNA: temporal changes following subarachnoid hemorrhage. *Physiol Genomics*. 2016;48:361–366.
36. Stylli SS, Adamides AA, Koldej RM, Luwor RB, Ritchie DS, Ziogas J, Kaye AH. miRNA expression profiling of cerebrospinal fluid in patients with aneurysmal subarachnoid hemorrhage. *J Neurosurg*. 2017;126:1131–1139.
37. Boo L, Ho WY, Ali NM, Yeap SK, Ky H, Chan KG, Yin WF, Satharasinghe DA, Liew WC, Tan SW, Ong HK, Cheong SK. MiRNA transcriptome profiling of spheroid-enriched cells with cancer stem cell properties in human breast MCF-7 cell line. *Int J Biol Sci*. 2016;12:427–445.
38. Sayagues JM, Corchete LA, Gutierrez ML, Sarasquete ME, Del Mar Abad M, Bengoechea O, Ferminan E, Anduaga MF, Del Carmen S, Iglesias M, Esteban C, Angoso M, Alcazar JA, Garcia J, Orfao A, Munoz-Bellvis L. Genomic characterization of liver metastases from colorectal cancer patients. *Oncotarget*. 2016;7:72908–72922.
39. Huang X, Yuan T, Liang M, Du M, Xia S, Dittmar R, Wang D, See W, Costello BA, Quevedo F, Tan W, Nandy D, Bevan GH, Longenbach S, Sun Z, Lu Y, Wang T, Thibodeau SN, Boardman L, Kohli M, Wang L. Exosomal miR-1290 and miR-375 as prognostic markers in castration-resistant prostate cancer. *Eur Urol*. 2015;67:33–41.
40. Mao Y, Liu J, Zhang D, Li B. MiR-1290 promotes cancer progression by targeting nuclear factor I/X(NFIX) in esophageal squamous cell carcinoma (ESCC). *Biomed Pharmacother*. 2015;76:82–93.
41. Zhang WC, Chin TM, Yang H, Nga ME, Lunny DP, Lim EK, Sun LL, Pang YH, Leow YN, Malusay SR, Lim PX, Lee JZ, Tan BJ, Shyh-Chang N, Lim EH, Lim WT, Tan DS, Tan EH, Tai BC, Soo RA, Tam WL, Lim B. Tumour-initiating cell-specific miR-1246 and miR-1290 expression converge to promote non-small cell lung cancer progression. *Nat Commun*. 2016;7:11702.
42. He XM, Zheng YQ, Liu SZ, Liu Y, He YZ, Zhou XY. Altered plasma microRNAs as novel biomarkers for arteriosclerosis obliterans. *J Atheroscler Thromb*. 2016;23:196–206.
43. Ding CF, Chen WQ, Zhu YT, Bo YL, Hu HM, Zheng RH. Circulating microRNAs in patients with polycystic ovary syndrome. *Hum Fertil (Camb)*. 2015;18:22–29.

SUPPLEMENTAL MATERIAL

Table S1. miRNA primer sets for qRT-PCR

miRNA	Forward primer sequence (5' to 3')	Reverse primer sequence (5' to 3')
hsa-miR-4433	GGAGCCAGTTGGACAG	GGTCCAGTTTTTTTTTTTTTTTATGTC
hsa-miR-93-5p	GCAAAGTGCTGTTCGTG	GTCCAGTTTTTTTTTTTTTTTCTACCT
hsa-miR-339-5p	CAGTCCCTGTCCTCCAG	GGTCCAGTTTTTTTTTTTTTTTCGT
hsa-miR-3651-5p	CATAGCCCGGTCGCT	GGTCCAGTTTTTTTTTTTTTTTCATGT
hsa-miR-27a	CAGTTCACAGTGGCTAAGTTC	CAGTTTTTTTTTTTTTTTGCGGAA
hsa-miR-27b	CAGTTCACAGTGGCTAAGTTC	TCCAGTTTTTTTTTTTTTTTGCAGA
hsa-miR-15a	CAGTAGCAGCACATAATGGT	GGTCCAGTTTTTTTTTTTTTTTCAC
hsa-miR-125a	CCCTGAGACCCTTTAACCT	GGTCCAGTTTTTTTTTTTTTTTCAC
hsa-miR-4454	GCAGGGATCCGAGTCAC	GGTCCAGTTTTTTTTTTTTTTTGGT
hsa-miR-132-3p	GCAGTAACAGTCTACAGCCA	GTCCAGTTTTTTTTTTTTTTTCGAC
hsa-miR-4463	GCAGGAGACTGGGGTG	GTTTTTTTTTTTTTTTGGCCCCAC
hsa-miR-324	AGAACATTCATTGTTGTCGGT	GGTCCAGTTTTTTTTTTTTTTTACAC
hsa-miR-421	GCAGATCAACAGACATTAATTGG	GTTTTTTTTTTTTTTTGCGCCCA
hsa-mir-4492	GGGCTGGGCGC	GTCCAGTTTTTTTTTTTTTTTGGC
hsa-miR-4793	TGCACTGTGAGTTGGCT	GGTCCAGTTTTTTTTTTTTTTTTAGC
hsa-miR-4689	CAGTTGAGGAGACATGGTG	GTTTTTTTTTTTTTTTGGCCCCCA
hsa-miR-4449	GGGGCTGCGCGA	TCCAGTTTTTTTTTTTTTTTGCCT
hsa-miR-1290	CGCAGTGGATTTTTGGATCA	GTCCAGTTTTTTTTTTTTTTTCCCT
hsa-miR-4497	TCCGGGACGGCTG	CCAGTTTTTTTTTTTTTTTGCCCA
hsa-miR-4690-5p	GAGCAGGCGAGGCT	GGTCCAGTTTTTTTTTTTTTTTCAG
hsa-miR-4459	GGAGGCGGAGGAGGT	GGTCCAGTTTTTTTTTTTTTTTCTC
hsa-miR-4674	GCTGGGCTCGGGAC	CCAGTTTTTTTTTTTTTTTAGCCG
hsa-miR-1268	GGGCGTGGTGGTG	GGTCCAGTTTTTTTTTTTTTTTCAC
hsa-miR-3178	GCGCGGCCGGA	GGTCCAGTTTTTTTTTTTTTTTCGAT
hsa-miR-297	GCAGATGTATGTGTGCATGTG	AGGTCCAGTTTTTTTTTTTTTTTCAT
hsa-miR-574	GTGAGTGTGTGTGTGTGAG	CAGGTCCAGTTTTTTTTTTTTTTTACA
hsa-miR-4532	CCCGGGGAGCCC	CAGTTTTTTTTTTTTTTTCGCCG
hsa-miR-4440	TCGTGGGGCTTGCT	CAGTTTTTTTTTTTTTTTCAAGCCA
cel-miR-39	GTCACCGGGTGTAAATCAG	CCAGTTTTTTTTTTTTTTTCAAGCTG

Table S2. Gene onthology and KEGG enrichment analyses of the targets of *miR-4532*, *miR-4463*, *miR-1290* and *miR-4793-3p*

MapID	MapTitle	Pvalue	AdjustedPv	x	y	n	N	EnrichDirect	GeneIDs
map04310	Wnt signaling pathway	0.004095503	0.521424353	5	20	61	1069	Over	ENST00000268459 ENST00000272164 ENST00000374806 ENST00000370828 ENST00000374694
map05217	Basal cell carcinoma	0.008067372	0.521424353	3	8	61	1069	Over	ENST00000272164 ENST00000297261 ENST00000374694
map05205	Proteoglycans in cancer	0.013642665	0.521424353	6	36	61	1069	Over	ENST00000559488 ENST00000272164 ENST00000297261 ENST00000264033 ENST00000355622 ENST00000374694
map04340	Hedgehog signaling pathway	0.015921354	0.521424353	3	10	61	1069	Over	ENST00000308595 ENST00000297261 ENST00000255641
map04924	Renin secretion	0.026893481	0.625634513	3	12	61	1069	Over	ENST00000374806 ENST00000245457 ENST00000368680
map04925	Aldosterone synthesis and secretion	0.028655016	0.625634513	2	5	61	1069	Over	ENST00000302909 ENST00000368680
map04724	Glutamatergic synapse	0.049227337	0.80639532	3	15	61	1069	Over	ENST00000308595 ENST00000382159 ENST00000374806
map04921	Oxytocin signaling pathway	0.049245516	0.80639532	4	25	61	1069	Over	ENST00000374806 ENST00000270458 ENST00000263026 ENST00000368680
map00750	Vitamin B6 metabolism	0.057062675	0.830578942	1	1	61	1069	Over	ENST00000225573
map04120	Ubiquitin mediated proteolysis	0.086326741	0.898333442	4	30	61	1069	Over	ENST00000399816 ENST00000492996 ENST00000264033 ENST00000291582
map04550	Signaling pathways regulating pluripotency of stem cells	0.100843751	0.898333442	3	20	61	1069	Over	ENST00000272164 ENST00000231121 ENST00000374694
map04745	Phototransduction - fly	0.110919583	0.898333442	1	2	61	1069	Over	ENST00000308595
map04122	Sulfur relay system	0.110919583	0.898333442	1	2	61	1069	Over	ENST00000452446
map04390	Hippo signaling pathway	0.113045039	0.898333442	3	21	61	1069	Over	ENST00000272164 ENST00000374694 ENST00000590071
map05412	Arrhythmogenic right ventricular cardiomyopathy (ARVC)	0.146390899	0.898333442	2	12	61	1069	Over	ENST00000559488 ENST00000270458
map04392	Hippo signaling pathway - multiple species	0.161747985	0.898333442	1	3	61	1069	Over	ENST00000590071
map03030	DNA replication	0.161747985	0.898333442	1	3	61	1069	Over	ENST00000308418
map04916	Melanogenesis	0.187886844	0.898333442	2	14	61	1069	Over	ENST00000272164 ENST00000374694
map05414	Dilated cardiomyopathy	0.187886844	0.898333442	2	14	61	1069	Over	ENST00000559488 ENST00000270458
map01100	Metabolic pathways	0.201576085	0.898333442	6	177	61	1069	Under	ENST00000225573 ENST00000216484 ENST00000244043 ENST00000339600 ENST00000340941 ENST00000258873
map05410	Hypertrophic cardiomyopathy (HCM)	0.209219076	0.898333442	2	15	61	1069	Over	ENST00000559488 ENST00000270458
map00910	Nitrogen metabolism	0.209715502	0.898333442	1	4	61	1069	Over	ENST00000454127
map00061	Fatty acid biosynthesis	0.209715502	0.898333442	1	4	61	1069	Over	ENST00000258873
map04976	Bile secretion	0.209715502	0.898333442	1	4	61	1069	Over	ENST00000261196
map00600	Sphingolipid metabolism	0.209715502	0.898333442	1	4	61	1069	Over	ENST00000216484
map04146	Peroxisome	0.230795625	0.898333442	2	16	61	1069	Over	ENST00000396385 ENST00000295030
map05032	Morphine addiction	0.230795625	0.898333442	2	16	61	1069	Over	ENST00000308595 ENST00000382159
map04145	Phagosome	0.242197418	0.898333442	3	30	61	1069	Over	ENST00000559488 ENST00000350896 ENST00000355622

map03022	Basal transcription factors	0.254980623	0.898333442	1	5	61	1069	Over	ENST00000607778
map05340	Primary immunodeficiency	0.254980623	0.898333442	1	5	61	1069	Over	ENST00000291582
map00514	Other types of O-glycan biosynthesis	0.254980623	0.898333442	1	5	61	1069	Over	ENST00000389617
map03013	RNA transport	0.274309765	0.898333442	2	18	61	1069	Over	ENST00000542526 ENST00000281950
map04660	T cell receptor signaling pathway	0.274309765	0.898333442	2	18	61	1069	Over	ENST00000374806 ENST00000264033
map04919	Thyroid hormone signaling pathway	0.296085044	0.898333442	2	19	61	1069	Over	ENST00000559488 ENST00000396671
map04978	Mineral absorption	0.2976932	0.898333442	1	6	61	1069	Over	ENST00000233202
map03440	Homologous recombination	0.2976932	0.898333442	1	6	61	1069	Over	ENST00000359321
map05031	Amphetamine addiction	0.2976932	0.898333442	1	6	61	1069	Over	ENST00000374806
map05134	Legionellosis	0.2976932	0.898333442	1	6	61	1069	Over	ENST00000355622
map04918	Thyroid hormone synthesis	0.2976932	0.898333442	1	6	61	1069	Over	ENST00000392256
map04341	Hedgehog signaling pathway - fly	0.2976932	0.898333442	1	6	61	1069	Over	ENST00000255641
map04720	Long-term potentiation	0.2976932	0.898333442	1	6	61	1069	Over	ENST00000374806
map04130	SNARE interactions in vesicular transport	0.2976932	0.898333442	1	6	61	1069	Over	ENST00000367568
map04020	Calcium signaling pathway	0.317778521	0.898333442	2	20	61	1069	Over	ENST00000282018 ENST00000374806
map04144	Endocytosis	0.318859077	0.898333442	4	45	61	1069	Over	ENST00000308595 ENST00000264033 ENST00000356956 ENST00000304032
map04080	Neuroactive ligand-receptor interaction	0.33714738	0.898333442	4	47	61	1069	Over	ENST00000282018 ENST00000590320 ENST00000245457 ENST00000396671
map04142	Lysosome	0.339329413	0.898333442	2	21	61	1069	Over	ENST00000233202 ENST00000356956
map04071	Sphingolipid signaling pathway	0.360683922	0.898333442	2	22	61	1069	Over	ENST00000216484 ENST00000590320
map03420	Nucleotide excision repair	0.376019682	0.898333442	1	8	61	1069	Over	ENST00000607778
map03008	Ribosome biogenesis in eukaryotes	0.376019682	0.898333442	1	8	61	1069	Over	ENST00000341162
map04215	Apoptosis - multiple species	0.376019682	0.898333442	1	8	61	1069	Over	ENST00000318407
map01212	Fatty acid metabolism	0.376019682	0.898333442	1	8	61	1069	Over	ENST00000258873
map05014	Amyotrophic lateral sclerosis (ALS)	0.376019682	0.898333442	1	8	61	1069	Over	ENST00000374806
map05144	Malaria	0.41189414	0.898333442	1	9	61	1069	Over	ENST00000355622
map00590	Arachidonic acid metabolism	0.41189414	0.898333442	1	9	61	1069	Over	ENST00000244043
map04662	B cell receptor signaling pathway	0.41189414	0.898333442	1	9	61	1069	Over	ENST00000374806
map04391	Hippo signaling pathway - fly	0.41189414	0.898333442	1	9	61	1069	Over	ENST00000590071
map04360	Axon guidance	0.422132398	0.898333442	3	32	61	1069	Over	ENST00000297261 ENST00000374806 ENST00000245323
map05200	Pathways in cancer	0.442258613	0.898333442	6	78	61	1069	Over	ENST00000382159 ENST00000272164 ENST00000297261 ENST00000264033 ENST00000245457 ENST00000374694
map03320	PPAR signaling pathway	0.445737967	0.898333442	1	10	61	1069	Over	ENST00000258873
map00071	Fatty acid metabolism	0.445737967	0.898333442	1	10	61	1069	Over	ENST00000258873
map04370	VEGF signaling pathway	0.445737967	0.898333442	1	10	61	1069	Over	ENST00000374806
map04922	Glucagon signaling pathway	0.445737967	0.898333442	1	10	61	1069	Over	ENST00000374806

map00280	Valine, leucine and isoleucine degradation	0.445737967	0.898333442	1	10	61	1069	Over	ENST00000340941
map04750	Inflammatory mediator regulation of TRP channels	0.445737967	0.898333442	1	10	61	1069	Over	ENST00000245457
map04114	Oocyte meiosis	0.445737967	0.898333442	1	10	61	1069	Over	ENST00000374806
map05152	Tuberculosis	0.454617174	0.902346208	3	36	61	1069	Over	ENST00000374806 ENST00000355622 ENST00000256458
map04010	MAPK signaling pathway	0.463909936	0.906592628	3	37	61	1069	Over	ENST00000265080 ENST00000374806 ENST00000270458
map04214	Apoptosis - fly	0.477664298	0.906592628	1	11	61	1069	Over	ENST00000318407
map05166	HTLV-I infection	0.504242149	0.906592628	3	41	61	1069	Over	ENST00000272164 ENST00000374806 ENST00000374694
map04923	Regulation of lipolysis in adipocytes	0.507780062	0.906592628	1	12	61	1069	Over	ENST00000368680
map05140	Leishmaniasis	0.507780062	0.906592628	1	12	61	1069	Over	ENST00000355622
map04920	Adipocytokine signaling pathway	0.507780062	0.906592628	1	12	61	1069	Over	ENST00000258873
map03015	mRNA surveillance pathway	0.536186321	0.906592628	1	13	61	1069	Over	ENST00000238714
map04512	ECM-receptor interaction	0.536186321	0.906592628	1	13	61	1069	Over	ENST00000559488
map04713	Circadian entrainment	0.562978588	0.906592628	1	14	61	1069	Over	ENST00000382159
map05133	Pertussis	0.562978588	0.906592628	1	14	61	1069	Over	ENST00000355622
map04727	GABAergic synapse	0.562978588	0.906592628	1	14	61	1069	Over	ENST00000382159
map05130	Pathogenic Escherichia coli infection	0.562978588	0.906592628	1	14	61	1069	Over	ENST00000355622
map03460	Fanconi anemia pathway	0.562978588	0.906592628	1	14	61	1069	Over	ENST00000294008
map04260	Cardiac muscle contraction	0.562978588	0.906592628	1	14	61	1069	Over	ENST00000270458
map05321	Inflammatory bowel disease (IBD)	0.562978588	0.906592628	1	14	61	1069	Over	ENST00000355622
map04721	Synaptic vesicle cycle	0.588247125	0.906592628	1	15	61	1069	Over	ENST00000263354
map04723	Retrograde endocannabinoid signaling	0.588247125	0.906592628	1	15	61	1069	Over	ENST00000382159
map04620	Toll-like receptor signaling pathway	0.588247125	0.906592628	1	15	61	1069	Over	ENST00000355622
map04726	Serotonergic synapse	0.588247125	0.906592628	1	15	61	1069	Over	ENST00000382159
map05100	Bacterial invasion of epithelial cells	0.612077225	0.921633523	1	16	61	1069	Over	ENST00000264033
map05012	Parkinson's disease	0.612077225	0.921633523	1	16	61	1069	Over	ENST00000339600
map05010	Alzheimer's disease	0.642889256	0.944927224	2	24	61	1069	Over	ENST00000374806 ENST00000339600
map04910	Insulin signaling pathway	0.656299976	0.944927224	2	26	61	1069	Over	ENST00000452015 ENST00000264033
map04022	cGMP-PKG signaling pathway	0.656299976	0.944927224	2	26	61	1069	Over	ENST00000374806 ENST00000368680
map04150	mTOR signaling pathway	0.663613012	0.944927224	2	27	61	1069	Over	ENST00000272164 ENST00000374694
map04380	Osteoclast differentiation	0.663613012	0.944927224	2	27	61	1069	Over	ENST00000559488 ENST00000374806
map04024	cAMP signaling pathway	0.687211007	0.96785942	2	30	61	1069	Over	ENST00000245457 ENST00000368680
map04062	Chemokine signaling pathway	0.695449691	0.96785942	2	31	61	1069	Over	ENST00000308595 ENST00000382159
map05034	Alcoholism	0.716617786	0.96785942	1	35	61	1069	Under	ENST00000382159
map04015	Rap1 signaling pathway	0.716617786	0.96785942	1	35	61	1069	Under	ENST00000559488

map04510	Focal adhesion	0.716659265	0.96785942	1	34	61	1069	Under	ENST00000559488
map04151	PI3K-Akt signaling pathway	1	1	3	60	61	1069	Under	ENST00000559488 ENST00000382159 ENST00000355622
map04066	HIF-1 signaling pathway	1	1	1	17	61	1069	Over	ENST00000355622
map04064	NF-kappa B signaling pathway	1	1	1	17	61	1069	Over	ENST00000355622
map05132	Salmonella infection	1	1	1	17	61	1069	Over	ENST00000355622
map00230	Purine metabolism	1	1	1	20	61	1069	Under	ENST00000368680
map04725	Cholinergic synapse	1	1	1	18	61	1069	Under	ENST00000382159
map04611	Platelet activation	1	1	1	23	61	1069	Under	ENST00000559488
map05142	Chagas disease (American trypanosomiasis)	1	1	1	20	61	1069	Under	ENST00000355622
map04270	Vascular smooth muscle contraction	1	1	1	18	61	1069	Under	ENST00000368680
map05145	Toxoplasmosis	1	1	1	31	61	1069	Under	ENST00000355622
map04014	Ras signaling pathway	1	1	2	42	61	1069	Under	ENST00000265080 ENST00000382159
map04931	Insulin resistance	1	1	1	18	61	1069	Under	ENST00000452015
map05206	MicroRNAs in cancer	1	1	1	23	61	1069	Under	ENST00000559488
map04932	Non-alcoholic fatty liver disease (NAFLD)	1	1	1	26	61	1069	Under	ENST00000339600
map05016	Huntington's disease	1	1	1	29	61	1069	Under	ENST00000339600
map04722	Neurotrophin signaling pathway	1	1	1	20	61	1069	Under	ENST00000256458
map04640	Hematopoietic cell lineage	1	1	1	18	61	1069	Under	ENST00000559488
map05162	Measles	1	1	1	18	61	1069	Under	ENST00000355622
map05323	Rheumatoid arthritis	1	1	1	25	61	1069	Under	ENST00000355622
map04530	Tight junction	1	1	1	31	61	1069	Under	ENST00000216181
map04740	Olfactory transduction	1	1	3	55	61	1069	Under	ENST00000308595 ENST00000382159 ENST00000315453
map04650	Natural killer cell mediated cytotoxicity	1	1	1	20	61	1069	Under	ENST00000374806
map04012	ErbB signaling pathway	1	1	1	20	61	1069	Under	ENST00000264033
map05164	Influenza A	1	1	1	26	61	1069	Under	ENST00000355622
map05161	Hepatitis B	1	1	1	21	61	1069	Under	ENST00000355622
map05146	Amoebiasis	1	1	1	18	61	1069	Under	ENST00000355622
map05202	Transcriptional misregulation in cancer	1	1	1	23	61	1069	Under	ENST00000296921
map04810	Regulation of actin cytoskeleton	1	1	2	41	61	1069	Under	ENST00000559488 ENST00000382108
map01120	Microbial metabolism in diverse environments	1	1	1	26	61	1069	Under	ENST00000225573
map04152	AMPK signaling pathway	1	1	1	20	61	1069	Under	ENST00000263026
map04261	Adrenergic signaling in cardiomyocytes	1	1	1	23	61	1069	Under	ENST00000270458
map00190	Oxidative phosphorylation	1	1	1	22	61	1069	Under	ENST00000339600
map05220	Chronic myeloid leukemia	1	1	1	19	61	1069	Under	ENST00000264033
map04728	Dopaminergic synapse	1	1	1	19	61	1069	Under	ENST00000382159